J. King Saud Univ., Vol. 2, *Eng. Sci.* (2), pp. 213–228 (1410H/1990)

Mathematical Model for Cyclic Loading of a R.C. Beam with Relocatable Plastic Hinges

Mohammad Shathly Al-Haddad
Assistant Professor, Department of Civil Engineering, King Saud University, P.O.Box 800, Riyadh–11421, Saudi Arabia

Abstract. A single component reinforced concrete beam element modified to include varying locations of plastic hinges, was developed for use in the DRAIN–2D computer program. The model simulates the major characteristics of a reinforced concrete beam subjected to load reversals. This model consists of an elastic line element, two inelastic rotational springs, and two rigid zones. The properties and function of each component are described in this paper. Also, a verification of its accuracy is given. The results indicated that the model is a good and an economical mathematical tool for simulating how relocation of a beam hinging zone affects the inelastic response of a reinforced concrete building under earthquake motion.

Introduction

In the last few years, a new design approach for beam-column joints in earthquake resistant reinforced concrete buildings has been explored. The idea of this new design concept is to move the beam hinging zone some distance away from the column face [1-4]. Theoretically, the joint will then be isolated from inelastic deformation and a reduction in the required joint transverse reinforcement could be anticipated. Such speculation has been subjected to several experimental investigations [1-4]. The experimental results have indicated a significant enhancement in the ductile hysteretic behavior of the reinforced concrete connection due to moving the beam hinging zone an appropriate distance away from the connection face. However, moving the beam hinging zone from its conventional location (column face) is anticipated to affect the dynamic response if a building subjected to earthquake excitation. In order to study the consequences of moving beam hinging zones away from the column face in the design of real buildings, there is a need for an idealized beam element model described in this paper and shown in Fig. 1.

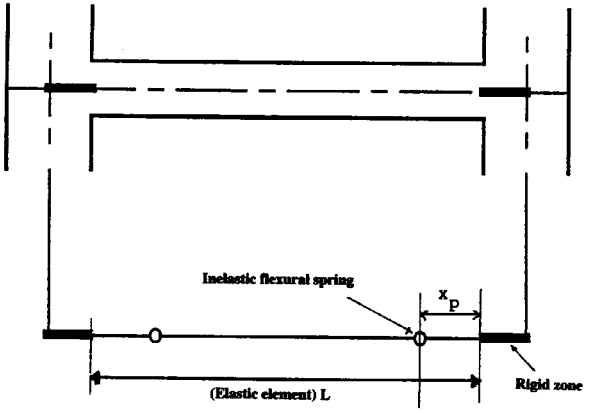

Fig. 1. Idealized beam element

Element Deformations

As was done for the beam-column and the original beam element in the DRAIN-2D program [5], the new beam element has three modes of deformation, namely axial extension and flexural rotation at each end (Fig. 2a). The relationship between the member incremental deformations {dv} and model incremental displacements {dr} (Fig. 2b) is as follows:

$$\{dv\} = [a] \{dr\} \tag{1}$$

where [a] is a displacement transformation matrix which is given in the DRAIN-2D report as follows:

$$[a] = \begin{bmatrix} -X/L & -Y/L & 0 & X/L & Y/L & 0 \\ -Y/L & X/L^2 & 1 & Y/L^2 & -X/L^2 & 0 \\ -Y/L^2 & X/L^2 & 0 & Y/L^2 & -X/L^2 & 1 \end{bmatrix} \tag{2}$$

Beam Model Components

The properties and functions of the components of the idealized beam, viz. the elastic line element, the flexural rotational springs, and rigid zones, are as follows.

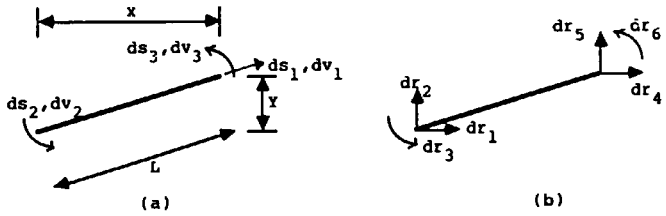

Fig. 2. Element end deformations and displacements

Elastic Line Element

The length of this component was assumed to be equal to the beam clear span (Fig. 1) and was intended to simulate beam elastic action. It also represented initial axial and flexural stiffness of the entire beam member. The axial stiffness (K_{11}) is given by:

$$ds_1 = \frac{EA}{L} \cdot dv_1 = K_{11}\ dv_1 \qquad (3)$$

in which:

ds_1 = the incremental axial force (Fig. 2a)

A = Equivalent cross sectional area

E = elastic modulus

L = length of the elastic line element

dv_1 = the incremental axial extension (Fig. 2a)

The elastic flexural stiffness in rotational degrees of freedom at each node is given by:

$$K_e = \frac{EI}{L} \begin{bmatrix} K_{22} & K_{23} \\ K_{32} & K_{33} \end{bmatrix} \qquad (4)$$

in which I = reference moment of inertia; and K_{22}, K_{33}, K_{32} and K_{23} are elastic flexural stiffness coefficients. The programmer must specify these coefficients and may account for such effects as shear deformation, non-rigid end connections, and cross section variations. For a member with a uniform moment of intertia, $K_{22} = K_{33} = 4$, and $K_{23} = 2$.

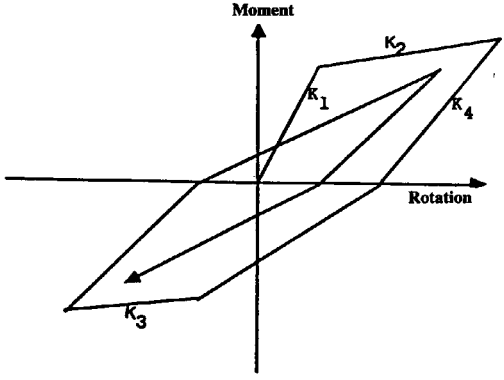

Fig. 3. Modified clough hysteresis model

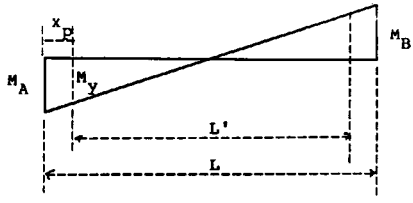

(a) Moment distribution

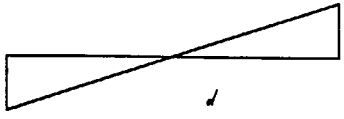

(b) Curvature distribution

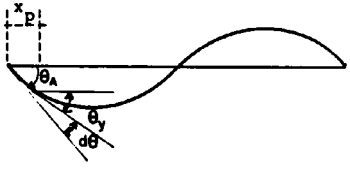

(c) Rotation

Fig. 4. Moment and rotation along member at yield level

Flexural Inelastic Rotation Springs

Rotational springs are positioned at the expected locations of the beam plastic hinging zones. The functions of these springs is to simulate inelastic action, if any, at these locations. The locations of the rotational springs can be varied. The moment vs. rotation relationship of the springs under load reversal was assumed to follow a modified version of the Clough's hysteretic model [6] shown in Fig. 3. The relationship is based on an idealized bilinear primary curve with an initial stiffness K_1 and a strain hardening stiffness K_2 beyond yielding. The initial stiffness is defined by calculating the coordinates of the yield point on the primary moment vs. rotation curve. To find the yield rotation the curvature distribution along the beam must be assumed. Here, the curvature was assumed to distribute linearly along the member, up to yield, with an inflection point at the beam mid-span (Fig. 4). This assumption about the location of inflection point was recognized to be fairly accurate for girders [7-11]. The spring rotation at the yield level can be calculated by applying moment-area theorems as follows:

$$\theta_y = \theta_A - d\theta \quad \text{(see Fig. 4)},$$

where

$$\theta_A = M_A \cdot L/6EI_{cr}$$

$$d\theta = (M_A + M_y) \cdot x_p/2EI_{cr}$$

Here, $M_A = M_y \cdot L/L'$ so that,

$$\theta_y = \frac{M_y L^2}{6L' \cdot EI_{cr}} - \frac{M_y[(1+L)/L']x_p}{2EI_{cr}} \tag{5}$$

where

θ_y = spring rotation at yield,

M_y = yield moment capacity of the section,

x_p = distance between the assumed location of the beam plastic hinge and the column face,

L = length of the elastic element,

L' = distance between the beam hinging zone $(L - 2x_p)$,

and

I_{cr} = cracked moment of inertia associated with the current direction of θ_y and M_y.

Then, the corresponding initial stiffness of the spring is,

$$K_1 = M_y/\theta_y \tag{6}$$

The strain hardening stiffness is specified as a ratio of the initial elastic stiffness as,

$$K_2 = pK_1 \tag{7}$$

The ratio p is specified by the program user.

The original Clough model provided for stiffness degradation only during the reloading stages. However, by virtue of its simple yet realistic representation, the Clough model has been widely used for inelastic analysis. Pursuant to this study, a basic modification to the original Clough model is made to provide for the softening of the stiffness in the unloading stages as well. The slope of the unloading branch, in Fig. 3, is defined as

$$K_4 = K_1 (\theta_y/\theta_{max})^{\gamma} \tag{8}$$

where

K_1 = slope of the elastic branch (Fig. 5)

θ_y = end rotation at yield level

θ_{max} = maximum end rotation during loading and,

γ = constant, assumed = 0.2 [12]

Rigid Zones

An infinitely rigid link was assumed at each end of the beam model. The function of this rigid zone is to simulate the beam-column joint core which is normally so designed to avoid formation of a plastic hinge within it. The method which was used to specify the rigid zone lengths, shown in fig.5, and to account for their effect in the analysis was exactly the same as for the beam-column element in DRAIN-2D. The displacement transformation relating the node displacements $\{dr_n\}$ with those at the ends of the elastic portion of the elements $\{d_r\}$ (Fig. 2b) is given in the DRAIN-2D user's guide as follows:

$$\begin{bmatrix} dr_1 \\ dr_2 \\ dr_3 \\ dr_4 \\ dr_5 \\ dr_6 \end{bmatrix} = \begin{bmatrix} 1 & 0 & -Y_i & 0 & 0 & 0 \\ 0 & 1 & X_i & 0 & 0 & 0 \\ 0 & 0 & 1 & 0 & 0 & 0 \\ 0 & 0 & 0 & 1 & 0 & -Y_j \\ 0 & 0 & 0 & 0 & 1 & X_j \\ 0 & 0 & 0 & 0 & 0 & 1 \end{bmatrix} \begin{bmatrix} dr_{1n} \\ dr_{2n} \\ dr_{3n} \\ dr_{4n} \\ dr_{5n} \\ dr_{6n} \end{bmatrix} \quad (9)$$

where X and Y are horizontal and vertical distances from the node to extremity of a rigid zone at i or j node as shown in Fig. 5. This transformation matrix is incorporated into the calculation of the element stiffnesses and deformations.

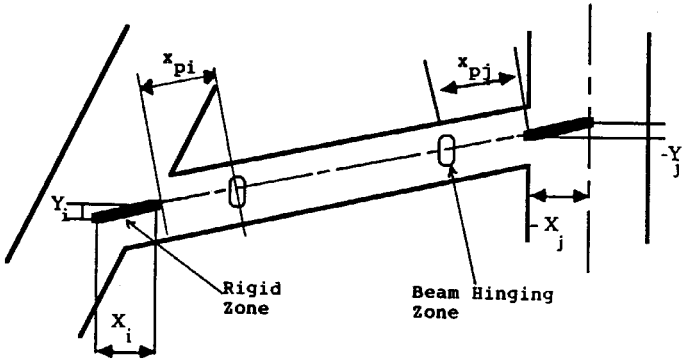

Fig. 5. Definition of rigid zone and locations of beam hinging zones

Member Stiffness

The new beam element possesses axial and flexural stiffness. The axial stiffness is represented by the elastic line element (Eq. 3). This axial stiffness remains unchanged. The flexural stiffness changes according to the loading status of the rotational springs. The current beam flexural stiffness is obtained by calculating and inverting its flexibility matrix. The member flexibility matrix is a combination of the elastic element flexibility matrix and the instantaneous flexibilities of the rotational springs. The elastic element flexibility matrix accounts for the member elastic flexural deformation and is obtained by inverting its stiffness matrix, given in Eq. 4, to get:

$$[F_e] = \begin{bmatrix} f_{11} & f_{12} \\ f_{12} & f_{22} \end{bmatrix} \tag{10}$$

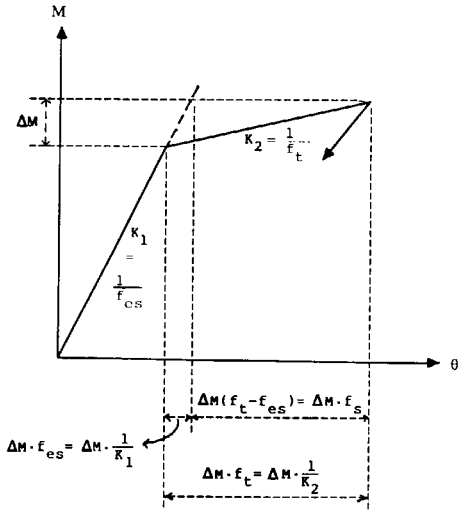

Fig. 6. Illustration for calculating the instantaneous flexibility of the rotational spring (f_s).

The instantaneous flexibilities of the rotational springs, which represent the member flexural inelastic action as illustrated in Fig. 6, is given by:

$$f_s = f_t - f_{es} \tag{11}$$

which

f_s = instantaneous flexibility of the rotational spring,

f_t = total flexibility of the spring which is defined by the hysteretic model,

f_{es} = elastic flexibility of the spring.

The components of the total member flexibility matrix are obtained by applying a unit moment separately at each end, as shown in Fig. 7, and using the virtual work concept as follows:

$$F_{11} = f_{11} + f_{s1}\,[1 - (x_p/L)]^2 + f_{s2}\,(x_p/L)^2$$
$$F_{12} = f_{12} - (f_{s1} + f_{s2})\,(x_p/L)\,[\,1 - (x_p/L)]$$
$$F_{21} = F_{12}$$
$$F_{22} = f_{22} + f_{s1}\,(x_p/L)^2 + f_{s2}\,[1 - (x_p/L)]^2$$

These equations can be rearranged and rewritten in the form:

$$[\,F\,] = [\,F_2\,] + [\,F_s\,] \qquad (12)$$

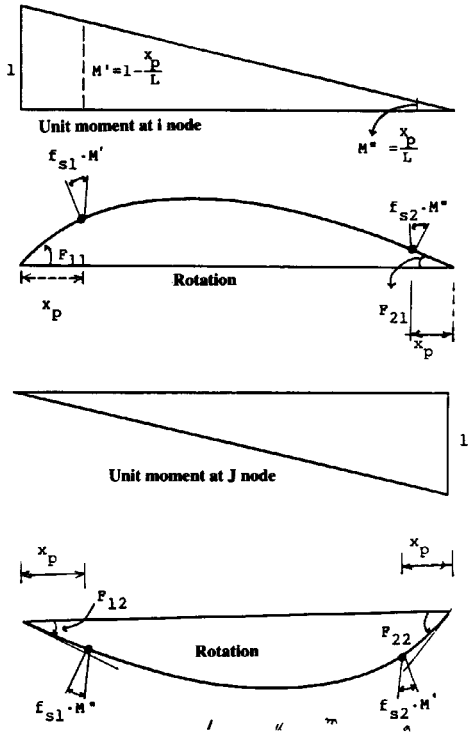

Fig. 7. Element rotation due to unit moment applied separately at each end

in which [F_e] is given by Eq. 10 and [F_s] is given by

$$[F_s] = [A]^T [F_s] [A] \tag{13}$$

where

$$[A] = \begin{bmatrix} 1-(x_p/L) & -x_p/L \\ -x_p/L & 1-(x_p/L) \end{bmatrix} \tag{14}$$

and

$$[f_s] = \begin{bmatrix} f_{s1} & 0 \\ 0 & f_{s2} \end{bmatrix} \tag{15}$$

in which f_{s1} and f_{s2} are calculated from Eq. 11. The incremental moments in the springs are related to the end moments shown in Fig. 2 as,

$$\begin{bmatrix} dM_{s1} \\ dM_{s2} \end{bmatrix} = [A] \begin{bmatrix} ds_2 \\ ds_3 \end{bmatrix} \tag{16}$$

The current moment stiffness matrix is obtained as $[k] = [F]^{-1}$.

The member stiffness matrix in global coordinates, { K_T }, is obtained by the coordinate transformation as,

$$[K_T] = [a]^T [K] [a]$$

Testing of the Element Model

To verify the accuracy and to check the logical mathematical formulation of the developed subroutines, two particular points needed verification. The first point was the ability of the subroutines to represent the desired hysteretic behavior of the rotational springs. The second point was the success of the subroutines in simulating the movements of the beam hinging zones. Tests of these two points are presented separately in the following sections.

Accuracy of the Hysteretic Behavior of the Beam Hinging Zone

During the output of results, five yield codes shown in Fig. 8 can be printed in order to show the beam end load and deformation level in accordance with the mod-

ified version of Clough's hysteretic model adopted here. Many printout statements were temporarily inserted during the development of the subroutines. These printouts were helpful to check whether the current yield code was the correct one for the current calculated load and deformation of the beam hinging zone. After a considerable effort using an example frame with three story, the results indicated that the printed yield codes correctly matched the calculated load levels at the hinging zone.

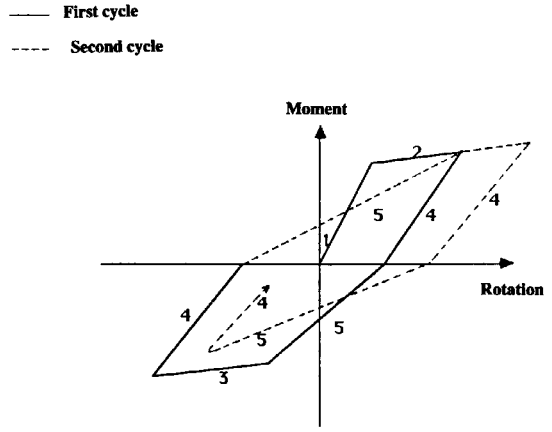

Fig. 8. Definition of output yield codes for the beam element model

During the parametric analysis of frames SDF1 and SDF2 (which are five story, two bay frames of 15 and 25 ft. span respectively) of the study described in references 12 and 13, computed hysteresis behavior of some selected beams was drawn in Figs. 9 and 10. It can be seen that the computed hysteretic behavior of the beam hinging zone closely matched the assumed hysteretic behavior shown in Fig. 8.

Accuracy of Simulating the Relocated Beam Hinging Zone

As explained previously, the new beam analytical model was intended to analytically move the beam hinging zone is the analysis. In other words, the beam can be idealized as one segment and the location of the hinging zone can be specified by the distance x_p shown in Fig. 5.

Moving the beam hinging zone, however, involved a difficult analytical modeling as explained by Eqs. 5–15. The accuracy of the model in simulating the movement

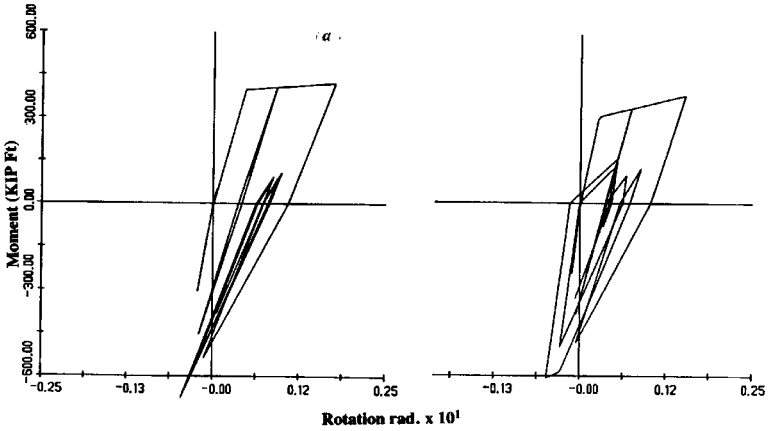

Fig. 9. Hysteretic responses of an interior beam hinging zone at level one of frame SDF1
(a) Beam which yielded at column face ,
(b) Beam which yielded at one beam depth away from the column face.

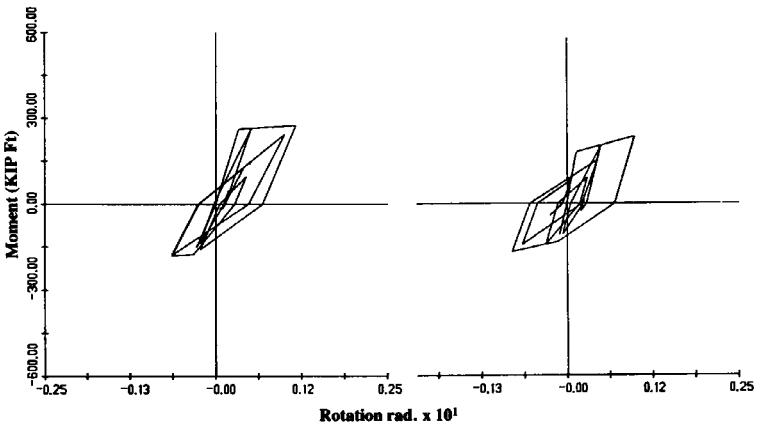

Fig. 10. Hysteretic response of an exterior beam hinging zone at level one of frame SDF2
(a) Beam which yielded at column face
(b) Beam which yielded at one beam depth away from the column face.

of hinging zone was verified by comparing its results to that of a beam which was essentially idealized by three segments as shown in Fig. 11. In particular, two test runs were performed using the first study frame SDF1 [13]. In the first run, the nodes were located at the joint centers and the beam was idealized as one segment. For this case, the entire beam was modelled by the new analytical beam model and the locations of the beam hinging zones were specified at one beam depth away from the column face (*i.e.*, $x_p = h$). For the other run, two more intermediate nodes were located at the moved hinging zones and the beam was idealized as three segments (Fig. 11). The parts between the column face and the moved hinging zones of segments 1 and 3 were modeled as perfectly elastic. Segment 2 was modeled by the new analytical model with hinging zones at its ends with $x_p = 0.0$, as explained in Fig. 11. The results of these two test runs are summarized in Table 1. It can be seen that the results for the two models were very similar.

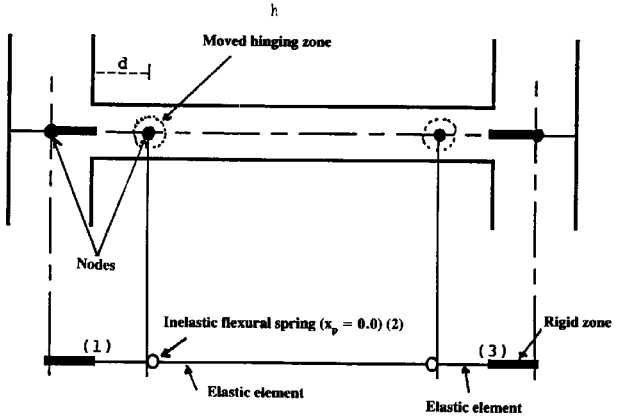

Fig. 11. Three segment beam idealization

Conclusions

The results of analysis using two models are essentially similar and historically the events of maximum responses occur at the same time in both models.

The time and cost of the calculation for the proposed one segment idealization of the beam (first run) was only about 40% of that for the three segments idealization (second run). It is, therefore, believed that the proposed beam element model is accurate and economical enough to simulate the effect of moving the beam hinging zone away from the column face during the dynamic response of a reinforced concrete building under earthquake motion.

Table 1. Comparison between the test runs for frame SDF1 with moved hinging zones*

Response parameter	Using the new beam model	Using three segments beam model
Maximum top floor displacement (in.)	6.8 (2.8)**	6.7 [2.8]
Maximum beam moment (k-ft.)	750 (2.89)	745 (2.89)
Maximum column moment (k-ft.)	937 (2.9)	937 (2.9)
Maximum beam rotational ductility	5.5 (2.89)	5.7 (2.89)
Maximum column rotational ductility	3.3 (2.9)	3.3 (2.9)
Maximum rotation of a first story interior joint (rad.10^{-3})	11.3 (2.89)	11.6 (2.89)

* See ref. [13] for description

** Values in parentheses are times of occurrence

References

[1] Galunic, B.; Bertero, V. and Popov, E. "An Approach for Improving Seismic Behavior of Reinforced Concrete Interior Joints." *Report No. EERC–77-30,* Earthquake Engineering Center, University of California, Berkeley, 1977.

[2] Paulay, T. and Park, R. "Joints in Reinforced Concrete Frames Designed for Earthquake Resistance." *Research Report No. 84–9,* Department of Civil Engineering, University of Christchurch, New Zealand, 1984.

[3] Abdel-Fattah, B.A. and Wight, J.K. "Experimental Study of Moving Beam Plastic Hinging Zones for Earthquake Resistant Design of R/C Buildings." *Report No. UMCE–85-11,* Department of Civil Engineering, University of Michigan, 1985.

[4] Wight, J.K.; Al-Haddad, M. and Abdel-Fattah, B. "Moving Beam Plastic Hinging Zone for Earthquake Resistant Design of R/C Buildings." *Proceedings of 3rd U.S. National Conference on Earthquake Engineering,* Charleston, S.C., August (1986).

[5] Kanaan, A.E. and Powell, G.H. "DRAIN-2D, A General Purpose Computer Program for Inelastic Dynamic Response of Plane Structures." *Report No. EERC–73-6,* Earthquake Engineering Research Center, University of California, Berkeley, 1973.

[6] Clough, R.W., "Effect of Stiffness Degradation on Earthquake Ductility Requirements." *Structures and Materials Research Report No. 66–16,* University of California, Berkeley, 1966.

[7] Giberson, M.F. "The Response of Nonlinear Multi-Story Structures Subjected to Earthquake Excitation." *Ph.D. Thesis,* California Institute of Technology, Pasadena, California, 1967.

[8] Otani, S. and Sozen, M.A. "Behavior of Multistory Reinforced Concrete Frames During Earthquake." *Civil Engineering Studies, Structural Research Series No. 392,* University of Illinois, Urbana, 1972.

[9] Otani, S. "SAKE-A Computer Program for Inelastic Response of R/C Frames to Earthquake." *Civil Engineering Studies, Structural Research Series No. 413,* University of Illinois, at Urbana-Champaign, November (1975).

[10] Saiidi, M. and Sozen, M. "Simple and Complex Models for Nonlinear Seismic Response of Reinforced Concrete Structures." *Civil Engineering Studies, Structural Research Series No. 465,* University of Illinois, Urbana, 1979.

[11] Banon, H.; Biggs, J. and Irvine, U. "Seismic Damage in Reinforced Concrete Frames." *Journal of Structural Division, ASCE,* 107, No. ST-9, (1981).

[12] Durrani, A.J. and Wight, J.K. "Experimental and Analytical Studies of Interior Reinforced Concrete Beam to Column Connections." *Report No. UMEE–82-R-3,* Department of Civil Engineering, University of Michigan, 1982.

[13] Al-Haddad, M.S. and Wight, J.K. "Feasibility and Consequences of Moving Beam Plastic Hinging Zones, for Earthquake Resistant Design of R/C Buildings." *Report No. UMCE–86-1,* Department of Civil Engineering, University of Michigan, 1986.

نموذج رياضي لكمرة خرسانة مسلحة تحت تأثير الأحمال الدورية مع إمكانية تحريك مناطق اللدونة

محمد شاذلي الحداد

قسم الهندسة المدنية، كلية الهندسة، جامعة الملك سعود، ص.ب ٨٠٠، الرياض ١١٤٢١، المملكة العربية السعودية

ملخص البحث. في هذا البحث تم تطوير نموذج رياضي لتمثيل كمرة الخرسانة المسلحة مع الأخذ في الاعتبار تحريك مناطق اللدونة بها، هذا النموذج يمثل الخصائص الرئيسة لكمرة الخرسانة المسلحة عند تعرضها إلى الأحمال المتغيرة الاتجاه. يتكون النموذج من عنصر مرن وزنبرك في كل طرف ذو حركة دوران غير خطية بالإضافة إلى منطقتين صلبتين، ولقد تم في هذا البحث وصف خصائص ووظيفة كل عنصر من هذه العناصر. ولقد دلت نتائج هذا البحث على أن هذا النموذج صحيح ويعتبر وسيلة جيدة واقتصادية لتمثيل تأثير تحريك مناطق اللدونة في الكمرات الخرسانية على حركة وتصرف المبنى عند تعرضه إلى الزلازل.